

Magnetic tunnel junctions with $L1_0$ -ordered FePt alloy electrodes

T. Moriyama ^{a)}

Institute for Materials Research, Tohoku University, Sendai 980-8577, Japan

S. Mitani ^{b)}

Institute for Materials Research, Tohoku University, Sendai 980-8577, and CREST, Japan Science and Technology Agency, Kawaguchi 332-0012, Japan

T. Seki

Institute for Materials Research, Tohoku University, Sendai 980-8577, Japan

T. Shima and K. Takanashi

Institute for Materials Research, Tohoku University, Sendai 980-8577, and CREST, Japan Science and Technology Agency, Kawaguchi 332-0012, Japan

A. Sakuma

Department of Applied Physics, Graduate School of Engineering, Tohoku University, Sendai 980-8579, Japan

(Presented on 7 January 2004)

Magnetic tunnel junctions (MTJs) with $L1_0$ -ordered FePt alloy electrodes were prepared on MgO(110) substrates, and structure and magnetotransport properties of the MTJs have been investigated. Tunnel magnetoresistance (TMR) of 34% is observed at 77 K for a junction with the FePt alloy electrode in which the degree of chemical order S is estimated to be ~ 0.7 . From S dependence of TMR in the MTJs, it is suggested that the spin polarization of FePt alloy electrodes increases with chemical ordering, which is consistent with first principles band structure calculations. © 2004 American Institute of Physics. [DOI:10.1063/1.1669212]

1. INTRODUCTION

Magnetic tunnel junction (MTJ) is a key structure in present and future spin electronics.¹ It is important to find electrode and barrier materials which are useful for the improvement in properties of MTJs. Recently, the problem of thermal fluctuation of magnetization has emerged in high-density magnetic recording, and also has become a general issue in nanometer-scale magnetic devices. $L1_0$ -ordered FePt alloy is a candidate ferromagnetic material that overcomes this problem because the magnetocrystalline anisotropy energy of $L1_0$ -ordered FePt reaches 7×10^7 erg/cc.² A great number of works on preparation,³⁻⁶ magnetic properties,⁶⁻⁸ and recording characteristics,^{4,9} etc. in $L1_0$ -ordered FePt have been performed to date. However tunnel magnetoresistance (TMR) has never been examined in any MTJ and granular film including $L1_0$ -ordered FePt alloys due to some difficulty in preparation of highly ordered $L1_0$ -FePt alloys in the film state. The FePt electrodes for MTJs in previous studies^{10,11} consist of Fe-rich disordered alloys. In this study, in-plane magnetized

$L1_0$ -ordered FePt films obtained in our recent experiment¹² were used for the electrodes in MTJs, and TMR and related properties of the MTJs have been investigated. In order to evaluate fundamental properties such as the sign of spin polarization and the chemical order dependence of TMR, simple sample structures have been chosen, i.e., the $L1_0$ -FePt alloys were used only for the bottom electrodes.

2. EXPERIMENTAL PROCEDURE

$\text{Fe}_{52}\text{Pt}_{48}$ bottom electrodes of 18 nm in thickness were sputter deposited on 10 nm thick Au(110) monocrystalline buffer layers grown on MgO(110) single crystal substrates. The substrate temperature T_s during FePt deposition was varied in the range from room temperature (RT) to 300 °C in order to change the degree of chemical order S in FePt. The reason for the use of Au(110) buffer layers is that well defined uniaxial magnetic anisotropy of the $L1_0$ -FePt layers is achieved in the in-plane direction (\parallel Au[001]).¹² The detailed growth conditions of the FePt layers were described in Ref. 12. To form a tunnel barrier, a 4.5 nm thick Al layer was deposited by sputtering at Ar pressure of 1.5 mTorr and was oxidized in oxygen-argon plasma for 10 min, where the oxygen-argon plasma was generated by applying 10 W rf power to 30 mTorr Ar-20% O₂ gas. The reason

^{a)} Present address: Dept. of physics and Astronomy, University of Delaware, DE.

^{b)} Author to whom correspondence should be addressed; electronic mail: mitani@imr.tohoku.ac.jp

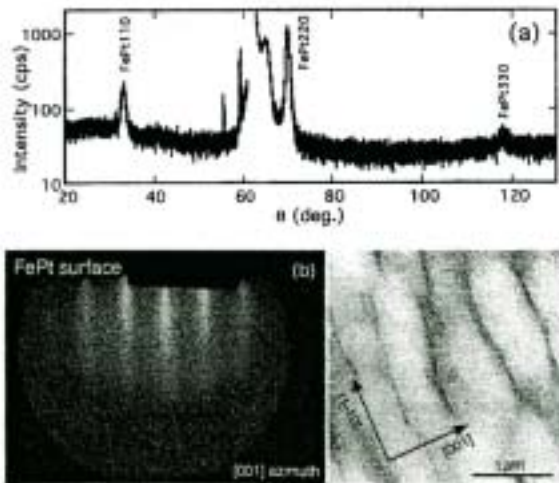


FIG. 1. (a) X-ray diffraction pattern of a FePt bottom electrode grown at 300 °C. (b) RHEED, and (c) AFM images of the film surface. The incident electron beam of the RHEED is along the MgO[100] direction.

for the use of unusually thick Al layers is that ohmic behavior was observed for most of MTJs with Al layers thinner than 4.5 nm. As a top electrode, a 20 nm thick $\text{Fe}_{20}\text{C}_{50}$ layer was deposited on the Al-O barrier by an electron beam evaporator. A couple of shadow masks of cross pattern were used for the samples of transport measurements where the junction area is $500 \times 500 \mu\text{m}^2$. X-ray diffraction (XRD), reflection high-energy electron diffraction (RHEED), and atomic force microscopy (AFM) observation were performed for structural characterization. Magnetic properties were measured for MTJs of $4 \times 4 \text{mm}^2$ with a superconducting quantum interference device magnetometer. Transport properties such as current-voltage (I - V) characteristics and TMR were measured by a conventional dc four-probe method. TMR ratio is defined as $(R_{\text{AP}} - R_{\text{P}}) / R_{\text{P}} \times 100(\%)$ in this article, where R_{P} and R_{AP} are the resistance of a MTJ in parallel and antiparallel alignments of magnetization of electrodes, respectively.

RESULTS AND DISCUSSION

Figure 1(a) shows the XRD pattern for a FePt bottom electrode grown at 300 °C. The FePt(110) peak associated with the $L1_0$ -type ordering is clearly observed. The degree of chemical order S evaluated from the intensity ratio of the superlattice peaks to the fundamental ones in the XRD pattern is 0.7 in the accuracy of ~ 0.1 . Since S decreases with decreasing T_s during the deposition of FePt layers, hereafter, the results for FePt grown at 300 °C are mainly shown. Surface roughness of the FePt electrodes is examined by RHEED and AFM. A typical RHEED image for a FePt electrode grown at 300 °C is shown in Fig. 1(b). The streak pattern indicates two-dimensional growth with high-density steps at the FePt surface. It is also confirmed from the RHEED image that the FePt electrode is monocrystalline. In contrast to the RHEED

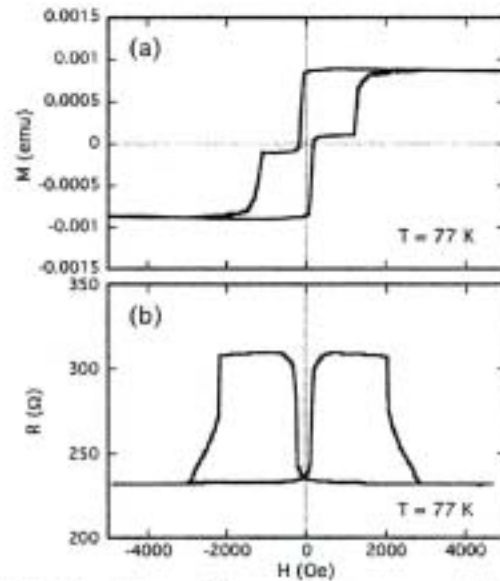


FIG. 2. (a) Magnetization and (b) magnetoresistance curves at 77 K for a MTJ with $L1_0$ -ordered FePt electrode grown at 300 °C.

image corresponding to the structure of nanometer scale, large roughness can be seen in the AFM image of $3 \times 3 \mu\text{m}^2$ for the FePt electrode [Fig. 1(c)]. Many large channels of $\sim 10 \text{nm}$ in depth are formed in the direction normal to $L1_0$ -FePt[001]. The large-scale roughness is probably due to the relatively large lattice mismatch between $L1_0$ -FePt and Au ($\sim 8\%$) and the substrate heating during deposition. The thick Al layers (4.5 nm) required to form pin-hole free tunnel barriers may be related to the observed roughness.

Figures 2(a) and 2(b) show the magnetization curve along the FePt[001] direction (easy magnetization axis) and the magnetoresistance curve, respectively, at 77 K for a MTJ with the ordered FePt electrode grown at 300 °C. Parallel and antiparallel alignments of the magnetization of FePt and FeCo electrodes are confirmed from the shape of the magnetization curve. The magnitude of the uniaxial magnetic anisotropy for the FePt film is estimated from the magnetization measurements to be $1.8 \times 10^7 \text{ erg/cc}$, which is about 2 orders of magnitude larger than those in Fe-Co alloys. The magnetoresistance curve exhibits a fairly large TMR ratio of 34%. The observed results imply that $L1_0$ -ordered FePt has a spin polarization comparable to that of pure Fe, although one may expect that the spin polarization of $L1_0$ -ordered FePt is considerably reduced by Pt atoms ($\sim 50 \text{ at. } \%$) having only a small magnetic moment ($0.3\text{--}0.4 \mu_B$).¹³ At RT, the TMR ratio is greatly reduced to 3.6% for the MTJ. The large temperature dependence is probably due to the fact that the deposition and oxidation conditions of Al layers on the FePt electrodes have not been optimized yet. Actually, the resistance of the MTJ is unusually lowered at RT, implying that leak current paths across the Al-O barrier work at RT.

Figures 3(a) and 3(b) show the I - V curve and the V dependence of TMR at 77 K for the MTJ shown in Fig. 2. From Simmons' equation,¹⁴ the barrier height and width are evaluated

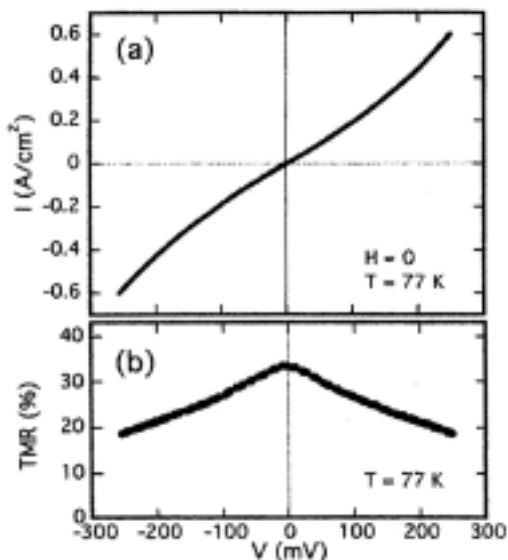


FIG. 3. (a) Current and (b) TMR as functions of bias voltage at 77 K for a MTJ with $L1_0$ -ordered FePt electrode grown at 300 °C.

to be 0.95 eV and 2.0nm, respectively. The evaluated barrier thickness is much smaller than the nominal thickness of the Al layers (=4.5nm). This indicates that the large thickness fluctuation exists in the Al layers and that the thickness of the thinner part of Al layers is around 2 nm. TMR gradually decreases with increasing bias voltage. Around $V=300\text{mV}$, the TMR ratio becomes a half value of that at zero bias. Both the I - V curve and the V dependence of TMR are symmetric in the sign of V , suggesting that the electronic structures are not significantly different between the FePt/Al-O and Al-O/FeCo interfaces.

Electronic structures generally change with the degree of chemical order in ordered alloys. Thus, a considerable influence of chemical ordering is expected on the spin polarization of FePt alloys. TMR at 77 K for the MTJs with FePt electrodes is shown as a function of S in Fig. 4. It is found that the observed TMR tends to increase with increasing S . Although other factors, r.g. interface roughness, that may be also changed with S should be taken into account in order to determine the S dependence of TMR precisely, the data in Fig. 4 suggest that the spin polarization of $L1_0$ -FePt alloys is enhanced by

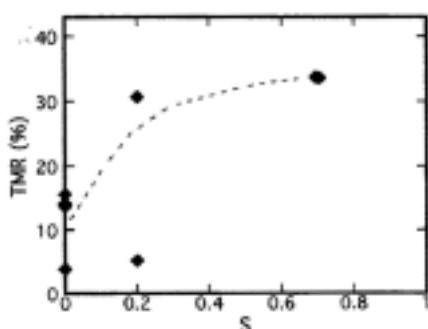


FIG. 4. Dependence of TMR on the degree of chemical order in FePt/Al-O/FeCo MTJs. The dashed line is a guide to the eye.

TABLE I. Spin polarizations of s and d electrons at the Fermi levels for $L1_0$ -ordered and disordered $\text{Fe}_{50}\text{Pt}_{50}$ alloys evaluated from the first principles band structure calculations.

	Spin polarization	
	s electron	d electron
$L1_0$ -ordered $\text{Fe}_{50}\text{Pt}_{50}$	+72%	-45%
Disordered $\text{Fe}_{50}\text{Pt}_{50}$	+29%	-26%

chemical ordering.

Finally, the observed TMR is discussed on the basis of first principles band structure calculation. TMR ratio is approximately given by $2P_1P_2/(1-P_1P_2)$ where P_1 and P_2 are the spin polarization of conduction electrons at Fermilevel for top and bottom electrodes,¹ and the spin polarization P can be evaluated from calculated band structure. Although this simple picture is not always true, it is considered that the TMR ratio correlates with P given by first principles band structure calculation. Calculated P values of s and d character electrons for $L1_0$ -ordered ($S=1$) and disordered ($S=0$) FePt alloys are shown in Table I. The calculation was based on the linear muffin-tin orbital method and local spin density approximation,¹³ and coherent phase approximation was used for the disordered alloy.¹⁵ Since the FePt/Al-O/FeCo MTJs do not show inverse TMR but a normal one, P of the FePt alloys should have the same sign as that in FeCo,¹ i.e., a positive. Therefore, the calculated P values of s electrons are important rather than those of d electrons, and are found to be comparable to P which is experimentally determined for Fe-Co-Ni alloys.¹ The most important point of the calculated results is that the P values of both s and d electrons are enhanced with chemical ordering. This is consistent with the observed S dependence of TMR for the MTJs with FePt electrodes.

CONCLUSION

We have investigated structure and magnetotransport properties of MTJs with $L1_0$ -ordered FePt alloy electrodes. TMR of 34% is observed at 77 K for a junction with the FePt alloy electrode in which S is estimated to be ~ 0.7 . It is also found that TMR of the MTJs with FePt alloy electrodes tends to increase with S , suggesting that P of $L1_0$ -FePt is enhanced by chemical ordering. The observed TMR ratios are consistent with the spin polarization evaluated from first principles band structure calculations.

ACKNOWLEDGMENT

This work was partly supported by IT-Program RR2002 from MEXT.

1. See for instance, T. Shinjo and S. Maekawa, *Spin Dependent Transport in Magnetic Nanostructures* (Taylor and Francis, London, 2002)
2. O. A. Ovanov, L. V. Solina, and V. A. Demshina, *Phys. Met. Metallogr.* **35**, 81(1973).
3. B. M. Lairson, M. R. Visokay, R. Sinclair, and B. M. Clemens, *Appl. Phys. Lett.* **62**, 639 (1993).
4. S. Sun, C. B. Murray, D. Weller, L. Folks, and A. Moser, *Science* **287**, 1989 (2000).
5. T. Shima, T. Moriguchi, S. Mitani, and K. Takanashi, *Appl. Phys. Lett.* **80**, 288 (2002).
6. A. Cebollada, R. F. C. Farrow, and M. F. Toney, in *Magnetic Nanostructures*, edited by H. S. Nalwa (American Scientific, Stevenson Ranch, CA, 2002), Chap. 3
7. J.-U. Thiele, L. Folks, M. F. Toney, and D. K. Weller, *J. Appl. Phys.* **84**, 5686 (1998).
8. S. Okamoto, N. Kikuchi, O. Kitakami, T. Miyazaki, Y. Shimada, and K. Fukamichi, *Phys. Rev. B* **66**, 024413 (2002).
9. T. Suzuki, H. Muraoka, Y. Nakamura, and K. Ouchi, *IEEE Trans. Magn.* **39**, 691 (2003).
10. J. S. Moodera and L. R. Kinder, *J. Appl. Phys.* **79**, 6262 (1996).
11. Y. Sugita, A. Odagawa, N. Matsukawa, Y. Kawashima, M. Satomi, Y. Morinaga, H. Adachi, and M. Hiramoto, *Jpn. J. Appl. Phys., Part 2* **41**, L1072 (2002).
12. T. Seki, T. Shima, and K. Takanashi, *J. Magn. Magn. Mater.* (in press).
13. A. Sakuma, *J. Phys. Soc. Jpn.* **63**, 3053 (1994).
14. J. G. Simmons, *J. Appl. Phys.* **34**, 1793 (1961).
15. A. Sakuma (unpublished).